# Application of a Necking Criterion to PET Fibers in Tension

**J. SWEENEY,[1] H. SHIRATAKI,[2] A. P. UNWIN,[3] I. M. WARD[3]**

[1] Department of Mechanical and Medical Engineering/IRC in Polymer Science and Technology, University of Bradford, Bradford BD7 1DP, United Kingdom

[2] Electronics Materials & Devices Laboratory, Asahi Chemical Industry Company Ltd., 2-1 Samejima Fuji Shizuoka 416-8501, Japan

[3] IRC in Polymer Science and Technology, University of Leeds, Leeds LS2 9JT, United Kingdom

*Received 13 January 1999; accepted 16 April 1999*

**ABSTRACT:** A criterion to predict instability in rate-dependent materials is developed. It is implemented for PET fibers in tension at three temperatures: 60, 75, and 80°C. At 60°C, necking is always observed, whereas at 80°C, the deformation is uniform, and 75°C marks a transition region, where necking is observed only at higher speeds and the deformation is otherwise uniform. As a necessary tool in the implementation of this criterion, the stress–strain behavior of PET is modeled using a combination of an Eyring process, a Gaussian network, and a linear elastic element. The resulting instability model gives predictions that are generally consistent with the experimental observations at all temperatures. © 1999 John Wiley & Sons, Inc. J Appl Polym Sci 74: 3331–3341, 1999

**Key words:** instability; necking; PET; mechanical behavior

## INTRODUCTION

There have been many studies of the stretching behavior of poly(ethylene terephthalate) (PET). These have been motivated by its commercial importance and the use of deformation processing to large strains to produce films and fibers. It is well established that rate-dependent yielding is a major aspect of its behavior,[1] as is the existence of a rubberlike network.[2] As with other polymers, attempts to fully define the mechanical behavior of PET require a constitutive equation comprising both network and yielding components.

An aspect of the behavior of PET which is especially important for this article is that it is capable both of cold-drawing with accompanying necking and of homogeneous deformation; the testing temperature and strain rate control which of these behaviors is observed. In physical terms, the mechanical properties of the material are the sole determinants of whether a neck is produced or not, with rate dependence being of particular significance. Criteria for neck growth can therefore be produced which are functions of the mechanical properties, and one such is discussed here. It is developed using minimum-energy arguments and its relationship with previously developed criteria is discussed. Its validity is explored in relation to predictions of necking for PET fibers at different temperatures. To assist this process, the mechanical behavior of the fibers is represented by a model, which includes both network and rate-dependent components.

## EXPERIMENTAL

The material examined here is a commercial grade of PET (Bright DEC, Asahi Chemical Ind., Samejima Fuji Shizuoka, Japan) containing

*Correspondence to:* J. Sweeney.

Journal of Applied Polymer Science, Vol. 74, 3331–3341 (1999)
 CCC 0021-8995/99/143331-11

0.06% $TiO_2$. The number-average molecular weight, from gel permeation chromatography, is 29,000. Melt-spun fiber was prepared using a take-up speed of 7.5 m $s^{-1}$; this is low enough to produce amorphous material with low molecular orientation. The fiber diameter was approximately 92 $\mu$m and the birefringence was less than $1.0 \times 10^{-3}$.

For the tensile experiments, specimens consisting of bundles of fibers containing 20 or 40 strands were used to ensure a measurable level of force. They were mounted between clamps, initially 50 mm apart, and drawn in an oven using an Instron testing machine. Tests were conducted at three temperatures, 60, 75, and 80°C, with air temperature controlled to within ±0.5°C. The samples were deformed at constant crosshead speeds, corresponding to overall strain rates $\dot{\lambda}$ in the range $6.67 \times 10^{-4}$ to $1.67 \times 10^{-1}$ $s^{-1}$, to a predetermined total elongation ratio of 3.0. Necking was detected by visual observation of the stretched specimens.

## THEORETICAL DEVELOPMENT OF NECKING CRITERION

The theoretical study of instabilities in solids was recently reviewed by van der Geissen and de Borst.[3] For materials for which stress is independent of the rate of strain, the shape of the stress–strain curve alone determines whether a tensile specimen will neck. For the true stress–strain curve, the Considere construction[4] can be applied and serves as the instability or necking criterion. When the material is characterized by the nominal or engineering stress as a function of strain, it can be shown that the equivalent criterion is the existence of a maximum in nominal stress, provided that the material is incompressible. Thus, for a curve like Figure 1, small and large strains, corresponding, respectively, to unnecked and necked material, can coexist in equilibrium. The nominal stress at which these strains coexist is less than the nominal stress corresponding to the homogeneous strain at the same extension, ensuring that the necked state represents a state of lower strain energy and that necking will always occur.

For rate-dependent materials, the position is more complex. The development of a neck will give rise to a locally high strain rate, which will cause a corresponding increase in stress. If the stress increase is too high, the necked specimen will no longer correspond to the lower stress and necking will not occur. In a rate-dependent material, the existence of a maximum on the nominal stress–strain curve is a necessary condition for necking, but not a sufficient one; if the rate dependence is too strong, necking is suppressed. Hart[5] analyzed the necking of tensile specimens of the rate-dependent material using a criterion based on the specimen cross-sectional area A. For a neck to occur, the instability condition was

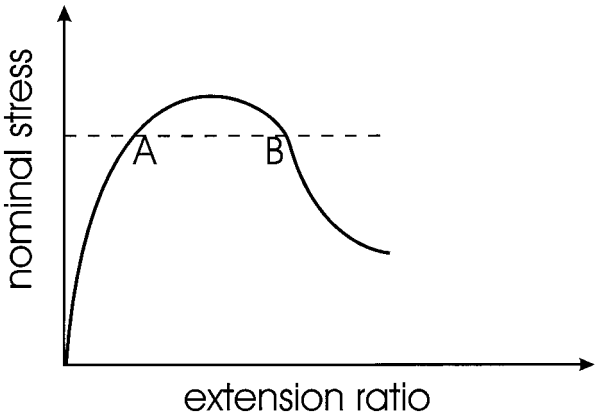


**Figure 1** Points A and B correspond to unnecked and necked material, respectively. They are at a stress lower than of the specimen when stretched homogeneously, for which the strain would be intermediate between the strains at the points A and B.

$$\left(\frac{\delta \dot{A}}{\delta A}\right)_S > 0 \tag{1}$$

where $\delta$ is a variation, the superposed dot denotes a time differential, and $S$ is the nominal stress. It seems intuitively plausible that this represents instability—a decrease in $A$ results in a decrease in the (negative) $\dot{A}$ and a further decrease in $A$. However, an equally plausible condition in terms of the extension ratio $\lambda$ and the true strain rate $\dot{\varepsilon} = \dot{\lambda}/\lambda$ was given by Coates and Ward[6] as

$$\frac{d\dot{\varepsilon}}{d\lambda} > 0 \tag{2}$$

which, since $d\lambda = \lambda d\varepsilon$ and $\lambda > 0$, is equivalent to

$$\frac{d\dot{\varepsilon}}{d\varepsilon} > 0 \tag{3}$$

Both (1) and (3) have the same intuitive appeal. To explore whether they are equivalent, let us

assume that the material is incompressible, so that

$$\lambda A = \exp(\varepsilon)A = 1$$

Then,

$$\frac{d\varepsilon}{dA} = -\frac{1}{A} \tag{4}$$

and

$$\dot{\varepsilon} = -\frac{\dot{A}}{A}$$

From the above equation, making use of (4), it follows that

$$\frac{d\dot{\varepsilon}}{d\varepsilon} = \left(\frac{\dot{A}}{A^2} - \frac{1}{A}\frac{d\dot{A}}{dA}\right)(-A) = \frac{d\dot{A}}{dA} - \frac{\dot{A}}{A}$$

Since $\dot{A}/A$ is, in general, nonzero, this shows that (1) and (3) are not equivalent. This holds true not only for the incompressible material considered here, but also, more generally, whenever $\lambda$ and $A$ are related by a time-independent factor. We shall explore this problem further by examining instability as a minimum-energy problem.

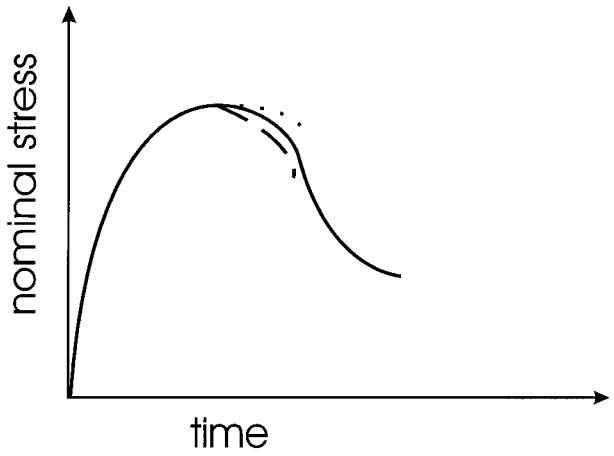


**Figure 2** Effect of an increase in strain rate at maximum nominal stress. The continuous curve represents a constant strain rate; the other lines increased rates. The dashed line corresponds to no or a relatively small rate dependence and to necking, since increasing the strain rate gives a lower stress. The dotted line represents a high rate dependence and the suppression of necking.

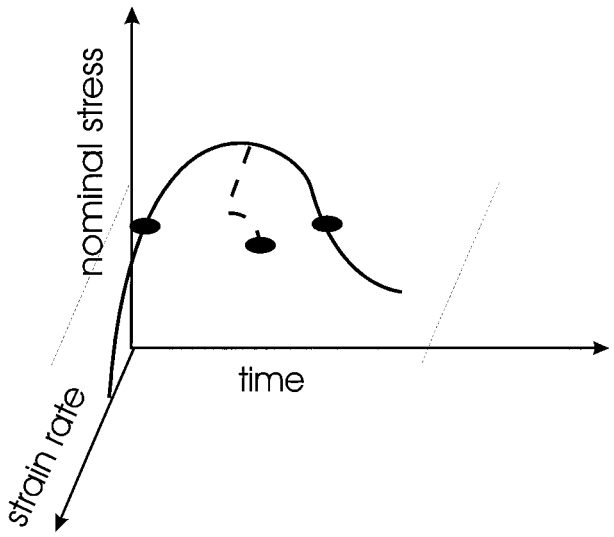


**Figure 3** The continuous curve is at constant strain rate. The dashed line corresponds to a strain rate that has been increased at the nominal stress maximum. In the case shown, the increased rate corresponds to a lower stress compared with the constant rate curve at the same time, and necking will occur.

When a material necks, the strain rate in the neck increases just after the nominal stress has reached its peak value. A rate increase at this point may either increase or decrease the stress relative to the value for an unchanged rate. This is shown in Figure 2, where nominal stresses are plotted against time. Where there is no rate dependence, increasing the rate at the nominal stress maximum will cause the stress at later times to be lower relative to that obtained at a constant rate. Therefore, increase in the rate will result in a lower stress and therefore a lower strain energy, and this condition corresponds to necking. As long as the rate dependence is not too high, the qualitative effect is the same and the specimen necks. However, when the rate dependence is so high that increasing the rate causes a relative increase in the nominal stress as a function of time, the least-energy condition corresponds to a constant rate and necking is suppressed. Our proposed instability criterion is thus that instability occurs whenever an increase in strain rate causes a drop in nominal stress as a function of time. Lower nominal stress ensures less energy input to the specimen, which is considered to be stretched at a constant overall strain rate.

To compare this criterion with those discussed so far, consider the nominal stress–time–strain rate surface for uniaxial deformation, shown in Figure 3. The case illustrated corresponds to in-

stability. At times after the peak in nominal stress, an increase in strain rate results in a nominal stress lower than that which would be obtained for continuing the deformation at the original strain rate. For a strain measure $e$ and its time derivative $\dot{e}$, with the original constant rate $\dot{e}_0$ and the perturbed rate $\dot{e}_1$, this corresponds to the condition for the nominal stress $S$

$$\left(\frac{\partial S}{\partial t}\right)_{\dot{e}_1} < \left(\frac{\partial S}{\partial t}\right)_{\dot{e}_0} < 0 \tag{5}$$

occurring just after the nominal stress maximum. In terms of strain rather than time, this becomes

$$\dot{e}_1\left(\frac{\partial S}{\partial e}\right)_{\dot{e}_1} < \dot{e}_0\left(\frac{\partial S}{\partial e}\right)_{\dot{e}_0} < 0$$

from which it follows that

$$\dot{e}_1\left[\left(\frac{\partial S}{\partial e}\right)_{\dot{e}_0} + (\dot{e}_1 - \dot{e}_0)\left(\frac{\partial^2 S}{\partial e\,\partial \dot{e}}\right)_{\dot{e}_0}\right] < \dot{e}_0\left(\frac{\partial S}{\partial e}\right)_{\dot{e}_0}$$

and

$$(\dot{e}_1 - \dot{e}_0)\left[\left(\frac{\partial S}{\partial e}\right)_{\dot{e}_0} + \dot{e}_1\left(\frac{\partial^2 S}{\partial e\,\partial \dot{e}}\right)_{\dot{e}_0}\right] < 0$$

For the onset of necking, we are interested in the situation at the maximum where the deformation is still essentially uniaxial and $[(\partial S)/(\partial e)]_{\dot{e}_0} = 0$, so that the criterion for necking becomes

$$(\dot{e}_1 - \dot{e}_0)\dot{e}_1\left(\frac{\partial^2 S}{\partial e\,\partial \dot{e}}\right)_{\dot{e}_0} < 0$$

This can be rewritten as

$$(\dot{e}_1 - \dot{e}_0)\dot{e}_1\left(\frac{\partial^2 S}{\partial e^2}\right)_{\dot{e}_0}\frac{de}{d\dot{e}} < 0 \tag{6}$$

For strain-rate measures that are positive in tensile deformation, the product $(\dot{e}_1 - \dot{e}_0)\dot{e}_1$ is clearly positive. For strain-rate measures that are negative in tension, an increase in the rate of tensile deformation will decrease the strain-rate measure, so that $\dot{e}_1 - \dot{e}_0 < 0$ and the product $(\dot{e}_1 - \dot{e}_0)\dot{e}_1$ remains positive. In either case, at the maximum $[(\partial^2 S)/\partial e^2)]_{\dot{e}_0} < 0$, and so (6) yields the condition

$$\frac{d\dot{e}}{de} > 0 \tag{7}$$

Relation (7) corresponds to a family of instability criteria, depending on the nature of the strain measure $e$, which includes conditions (1) and (3). It has been assumed that, as the peak nominal stress is approached, the rate of strain is constant. Therefore, conditions (1) and (3) correspond to different strain histories, since a constant area rate $\dot{A}$ corresponds to a decreasing true strain rate $\dot{\varepsilon}$. In many cases, when tensile tests are carried out at constant speeds, $\dot{\lambda}$ is initially constant and the appropriate strain measure is $e = \lambda$.

For computational purposes, we use the procedure illustrated in Figure 2. Nominal stress is calculated for constant strain rate $\dot{\lambda}$, corresponding to the constant speed testing condition. Then, using the same material parameters, it is calculated for a strain history for which the rate is kept constant up to the nominal stress maximum and then increased. The nominal stresses after the maximum are compared at the same instant of time, and necking is predicted when the stress corresponding to the perturbed rate is less than that corresponding to the constant rate. This method is applicable for any constitutive material behavior in which the stress may depend on the strain-rate history in a general way. The arguments or method used here do not, for instance, require the assumption that the stress be a function of only the current strain and strain rate as in previous studies,[6] nor that the strain rate depends only on the current stress and plastic strain.[7]

## STRESS–STRAIN CURVES: RESULTS AND MODELING

Results at the three temperatures, 60, 75, and 80°C, are discussed here. The major distinction between the highest and lowest temperature is that the fibers deform uniformly at 80°C whereas necking is observed at 60°C; this conforms with the findings of Rietsch et al.[8] and is related to the glass transition at around 70°C. The homogeneous deformation at the highest temperature enables the experiments to be interpreted directly as stress–strain curves. At 75°C, deformation is uniform at low strain rates and necking is observed at higher rates.

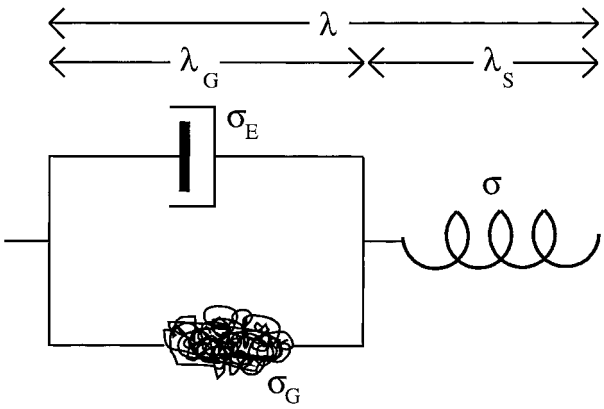


**Figure 4** Schematic diagram of model.

The model used is for uniaxial tension only and consists of three elements arranged as in Figure 4. The dashpot represents an Eyring process in which strain rate $\dot{\varepsilon}$, defined as above by

$$\dot{\varepsilon} = \frac{\dot{\lambda}_G}{\lambda_G}$$

is related to the true stress $\sigma_E$ by

$$\dot{\varepsilon} = A \sinh\left(\frac{\sigma_E v}{kT}\right) \tag{8}$$

where $A$ is a constant; $v$, the activation volume; $k$, Boltzmann's constant, and $T$, the absolute temperature. For the stress in terms of the strain rate, (8) becomes

$$\sigma_E = \frac{kT}{v} \ln\left[\frac{\dot{\varepsilon}}{A} + \sqrt{\left(\frac{\dot{\varepsilon}}{A}\right)^2 + 1}\right] \tag{9}$$

In this version of the Eyring process, a single activation volume is used, rather than the separate shear and pressure-activation volumes as used by Buckley and Jones[9] and Buckley et al.[10] Our simplified approach gives an adequate model of the stress–strain behavior.

In the opposite arm is a Gaussian network, in which the stress $\sigma_G$ is given by

$$\sigma_G = G(\lambda_G^2 - \lambda_G^{-1}) \tag{10}$$

where $G$ is a constant. The stresses $\sigma_E$ and $\sigma_G$ add together to give the total stress $\sigma$, which is itself equal to the stress in the third (spring) element. Thus,

$$\sigma = \sigma_G + \sigma_E \tag{11}$$

The total extension ratio $\lambda$ is multiplicatively decomposed into the spring extension $\lambda_S$ and the network and dashpot extension $\lambda_G$:

$$\lambda = \lambda_S \lambda_G \tag{12}$$

Finally, the total stress is related linearly to the true strain in the spring via the modulus $E$:

$$\sigma = E \ln \lambda_S \tag{13}$$

Stresses are calculated using an incremental procedure in which $\lambda$ is increased at an imposed rate. At each time increment, the value of $\lambda_G$ is calculated on the basis that the equilibrium eq. (11) is satisfied. Terms in this equation are evaluated using relations (9), (10), and (13). The strain rate $\dot{\varepsilon}$ in (9) is calculated from the backward difference in $\lambda_G$, and $\lambda_S$ in (13) is deduced using (12).

Results are presented in terms of nominal stress $S$. We assume the material to be incompressible, so that the true and nominal stresses are related by

$$S = \sigma/\lambda.$$

Haward[11] used a parallel combination of a Gaussian network and an Eyring process to model tensile polymer deformation. His model differs from that presented here in that it lacks the spring element; the effects of this component are mainly seen in the initial low-strain response, which was explicitly excluded from his study. There are several models of polymer deformation which have a general arrangement of components similar to that of Figure 4,[9,12,13] but which differ from it in the specific nature of the networks and viscous processes. The details of our model have been specified on grounds of simplicity and are such as to provide an adequate representation of the uniaxial deformations studied here.

### Results at 80°C

Figure 5 shows a typical nominal stress–extension ratio curve, for the strain rate $6.67 \times 10^{-3}$ $s^{-1}$. The observed stress is an average of three tests. Also shown is the theoretical curve using the model described above and the parameters of Table I. The major characteristic is the initial peak in stress. Note that, for this particular rate,

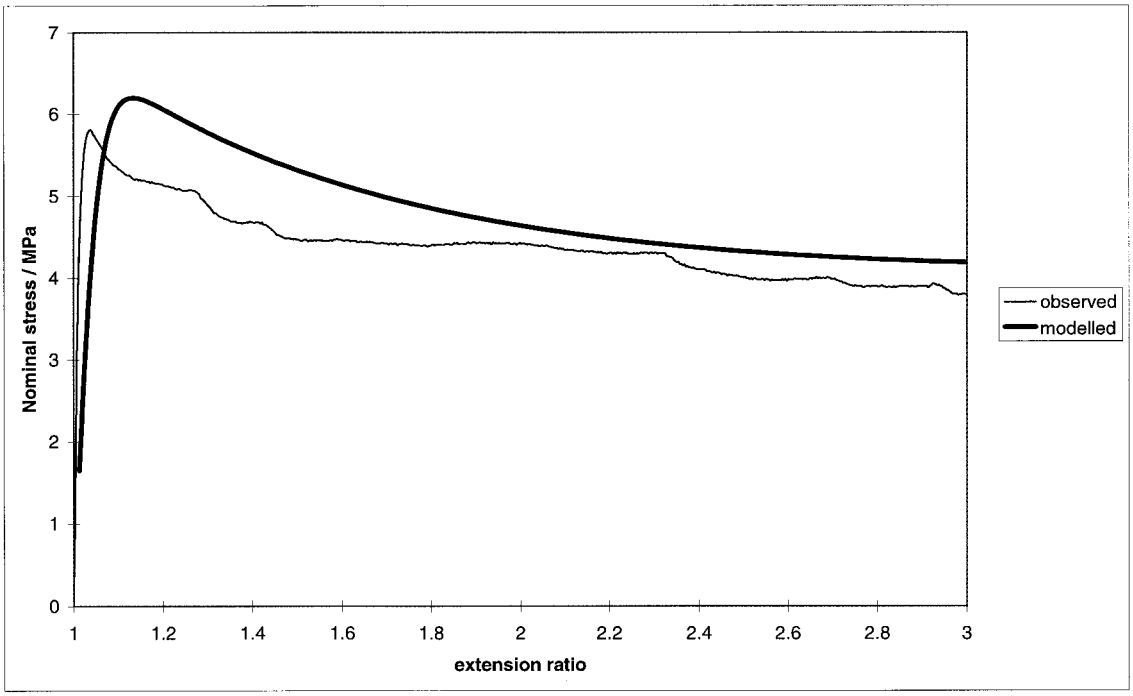


**Figure 5** Stress–strain curves at 80°C and strain rate $6.67 \times 10^{-3}$ $s^{-1}$.

slightly different parameters would give a closer prediction of the peak stress; however, the values in Table I were chosen to give a good fit for all the strain rates. The value of the modulus $E$ is deduced from the initial response at the higher testing speeds. The value of $A$ controls the height of the peak stress, and $v$ is derived from the rate dependence of the peak. The network parameter $G$ affects the stress level at high strains. Thus, the four parameters have distinct effects and so can be estimated without the use of sophisticated curve-fitting procedures.

The predicted and observed rate dependence of nominal stress at yield is shown in Figure 6. The model gives a good representation of the rate dependence; this is of crucial importance for its use in determining necking criteria. The rate dependence shown here defines the value of $v$. The value derived for $v$ can be compared with the values of pressure and shear activation volumes of Buckley et al.[10] which were obtained for PET at 87°C. In their more general Eyring theory, eq. (8) is replaced by

**Table I Model Parameters at 80°C**

| $E$ (GPa) | $A$ ($s^{-1}$) | $v$ (Å$^3$) | $G$ (MPa) |
|---|---|---|---|
| 0.15 | $9.0 \times 10^{-4}$ | 1660 | 0.8 |

$$\dot{\varepsilon} = A' \sinh\left(\frac{1}{2}\,\tau_{\text{oct}}\,\frac{v_S}{kT}\right)/\exp\left(-\bar{\sigma}\,\frac{v_p}{kT}\right) \quad (14)$$

where $v_s$ and $v_p$ are the shear and pressure-activation volumes, respectively; $\tau_{\text{oct}}$, the octahedral shear stress; and $\bar{\sigma}$, the mean stress. For a uniaxial tension $\sigma$, $\tau_{\text{oct}} = (\sqrt{2}/3)\sigma$ and $\bar{\sigma} = \frac{1}{3}\sigma$. Then, eq. (14) becomes

$$\dot{\varepsilon} = A' \sinh\left(\frac{1}{3\sqrt{2}}\,\frac{\sigma v_S}{kT}\right)/\exp\left(-\frac{\sigma v_P}{3kT}\right) \quad (15)$$

The values of shear and pressure-activation volumes are given[10] as $v_s = 7.23 \times 10^{-3}$ (12,000 Å$^3$) and $v_p = 1.35 \times 10^{-3}$ m$^3$/mol (2240 Å$^3$), respectively. Since $v_p \ll v_s$, the sinh function is the more strongly varying factor in eq. (15). We can therefore examine the compatibility of the activation volume in eq. (8) and Table I by comparing the sinh functions in eqs. (8) and (15); thus, $v = 1.0 \times 10^{-3}$ m$^3$/mol (1660 Å$^3$) is compared with $v_s/(3\sqrt{2}) = 1.7 \times 10^{-3}$ m$^3$/mol (2820 Å$^3$). This rough comparison shows a degree of consistency.

The network parameter $G$ can be interpreted in terms of the number of entanglements per unit volume $N$, via the relation $G = NkT$, where $k$ is Boltzmann's constant, and $T$, the absolute temperature. On this basis, the value in Table I of 0.8 MPa corresponds to $N = 1.64 \times 10^{26}$ m$^{-3}$. This

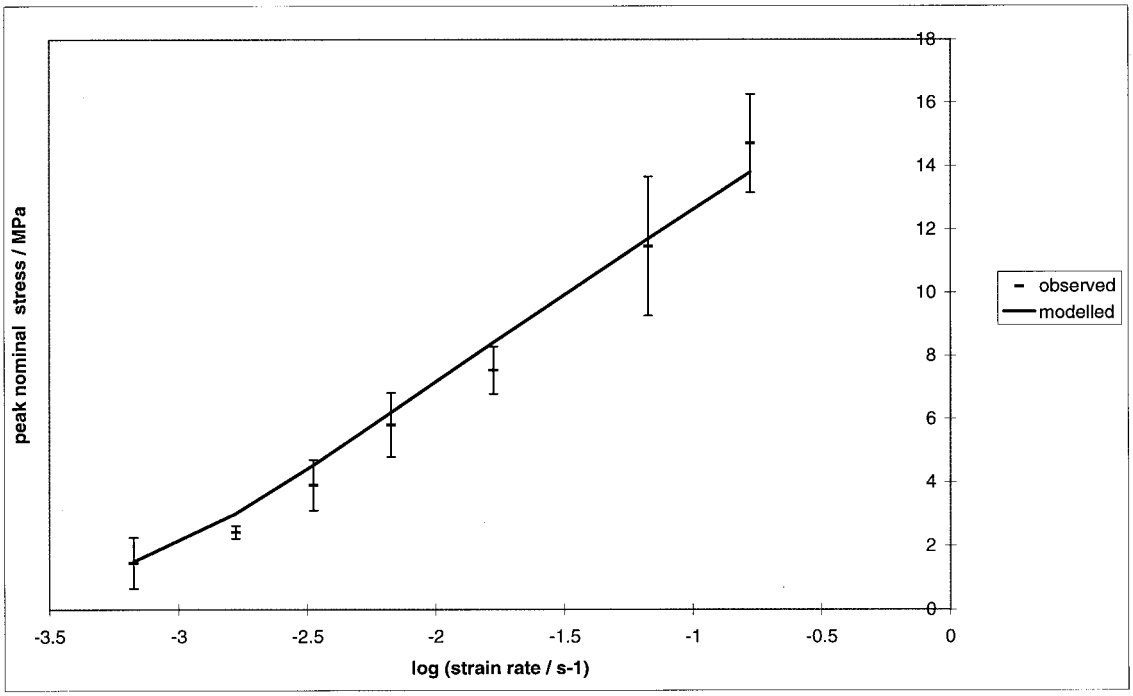


**Figure 6** Rate dependence of yield stress at 80°C.

is in good agreement to the value quoted by Buckley and Jones[9] ($1.67 \times 10^{26}$ $m^{-3}$) and reasonably consistent with other values[2,8] obtained in investigations above the glass transition temperature.

The shapes of the stress–strain curves at different strain rates are essentially the same as in Figure 5, except at the lowest rate of $6.67 \times 10^{-4}$ $s^{-1}$, where there is no peak in stress at yield. This is shown in Figure 7. The qualitative difference in behavior is captured by the model curve, which also shows no initial peak, but rather a change in slope at $\lambda \approx 1.1$. The stress at this point is taken as the "yield stress" plotted in Figure 6.

### Results at 60 and 75°C

When the fibers neck, load-extension curves cannot be simply associated with stress–strain curves, as the strain is inhomogeneous in the conditions prevailing after the load peak. However, we generated model curves using the theory set out above even when necking is observed. The stress–strain information up to the peak stresses is available as at 80°C, since deformation is uniform up to this point, so that $E$, $A$, and $v$ can be estimated as before. The network parameter $G$ is less readily accessible, since it contributes to the stress significantly only at high strains. However, for this reason, it is relatively unimportant for the purposes of neck prediction, since necks initiate at the stress peak. The values chosen are such as to give approximately the correct stress prediction at the natural draw ratio (i.e., when the strain is homogeneous again). This occurs at a draw ratio of approximately 3.5. Under ideal conditions of steady-state neck propagation, the strain in the necked part of the specimen stays constant at the natural draw ratio and the specimen elongates as the neck propagates into the unnecked region. During this process, the applied nominal stress remains constant. It is this value of stress that we observe experimentally and associate with the natural draw ratio.

Figure 8 shows the experimental load-extension curve at 60°C for the strain rate $6.67 \times 10^{-3}$ $s^{-1}$. This shows the approximately constant level of stress which is obtained after the peak. Since the load-extension curves are not simply related to stress–strain curves, no direct validation of the model is possible. However, the rate dependence of the peak can be compared with the model prediction, and this is done in Figure 9, where the model prediction is generated using the parameters of Table II. The rate dependence of the stress, when considered as a proportion of the total, is clearly weaker than at 80°C.

Similarly, in Table III, we show model parameters for the tests at 75°C. The associated predic-

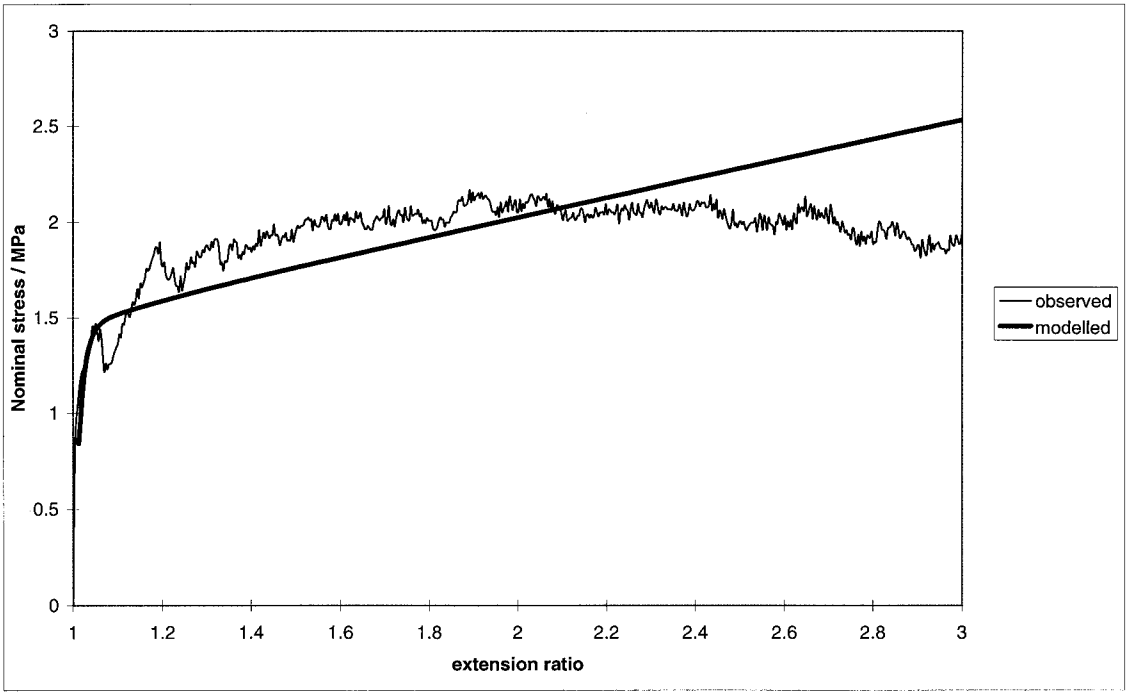


**Figure 7** Stress–strain curves at 80°C and strain rate $6.67 \times 10^{-4}$ $s^{-1}$.

tions of peak nominal stress are compared with observations as a function of testing rate in Figure 10.

It is apparent from the results of Tables I–III that the Gaussian parameter $G$ decreases with increasing temperature. $G$ only has significance at large strains, and the values used are such as to give realistic values of stress at and near the natural draw ratio. From the point of view of small-strain behavior, which is most relevant to

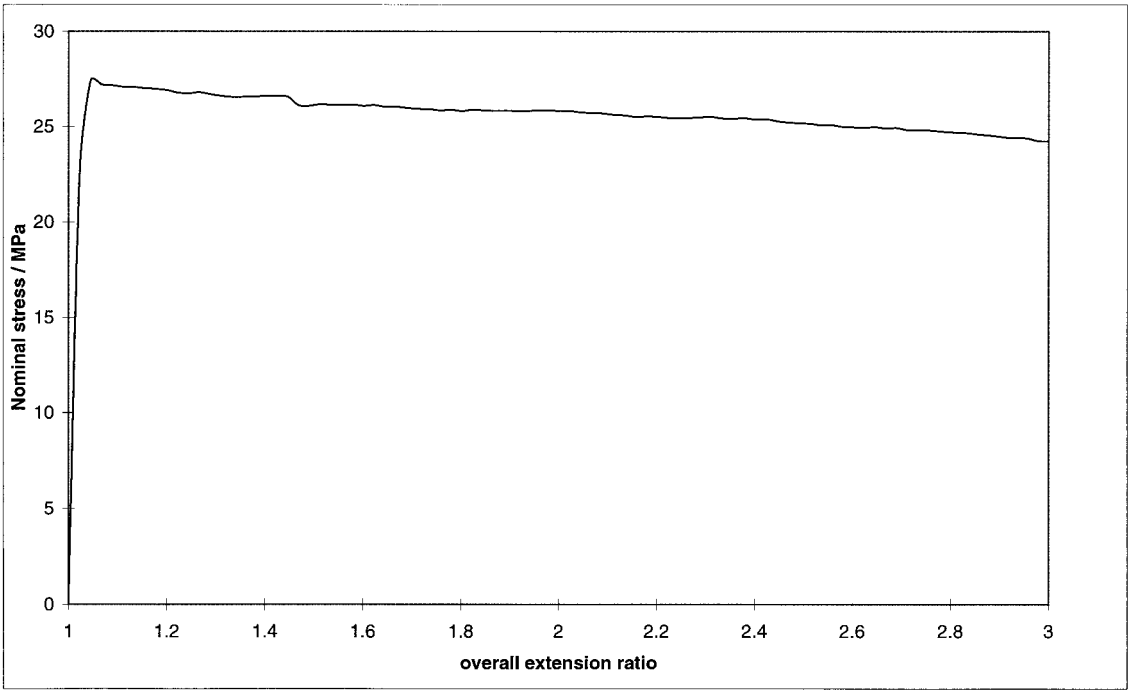


**Figure 8** Load-extension curve at 60°C and strain rate $6.67 \times 10^{-3}$ $s^{-1}$.

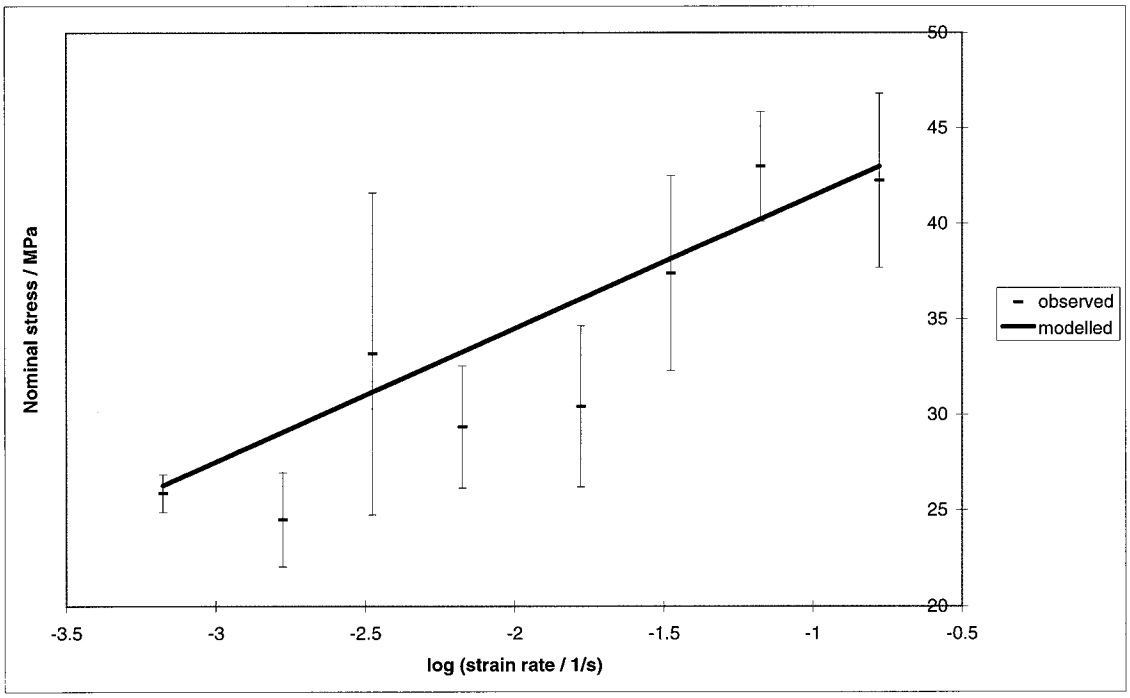


**Figure 9** Rate dependence of yield stress at 60°C.

the neck initiation characteristics studied here, $G$ is largely irrelevant. It has been confirmed that the necking predictions are the same when a value of $G$ which is constant with temperature, and equal to that of Table I, is used. However, stresses at large strain at 60 and 75°C are then underpredicted. The material is certainly stiffer at lower temperatures; this could be interpreted in terms of lower free volume below the glass transition, resulting in more chain–chain interactions. This is consistent with measurements of birefringence on samples drawn at different temperatures straddling the glass transition. Rietsch et al.[8] showed that the classical entanglement density, $N$, decreases as the drawing temperature is increased through the glass transition.

## NECKING PREDICTIONS

Using the constitutive model outlined in the previous section, stresses can be calculated for arbitrary strain-rate histories. It is used in the procedure for calculating the necking criterion described above. For each temperature and strain rate, the stress is calculated for a constant strain rate $\dot{\lambda}$ to determine the maximum nominal stress $S$ and the corresponding value of $\lambda$, to an accuracy $\delta\lambda = 10^{-5}$. The nominal stress is then calculated for a time $\Delta t$ after the attainment of the peak, for two cases: (i) where the strain rate is kept throughout at the original rate $\dot{\lambda}$, to give a stress $S_1$; and (ii) where the strain rate is kept to the original rate $\dot{\lambda}$ until the maximum nominal stress is reached, and then increased to $\dot{\lambda} + \Delta\dot{\lambda}$, to give a stress $S_2$. Necking is predicted to occur when $S_2 < S_1$.

The necking criterion is computed for each temperature and for the range of strain rates. In each case, the time increment $\Delta t$ corresponds to a change in $\lambda$ of 0.002 at the applied strain rate $\dot{\lambda}$. This level of change was chosen as sufficiently large so that the results are not dominated by round-off error, but small enough to be consistent

**Table II Model Parameters at 60°C**

| $E$ (GPa) | $A$ ($s^{-1}$) | $v$ (Å$^3$) | $G$ (MPa) |
|---|---|---|---|
| 2.0 | $2.0 \times 10^{-7}$ | 1440 | 4.0 |

**Table III Model Parameters at 75°C**

| $E$ (GPa) | $A$ ($s^{-1}$) | $v$ (Å$^3$) | $G$ (MPa) |
|---|---|---|---|
| 0.833 | $1.4 \times 10^{-4}$ | 1510 | 1.80 |

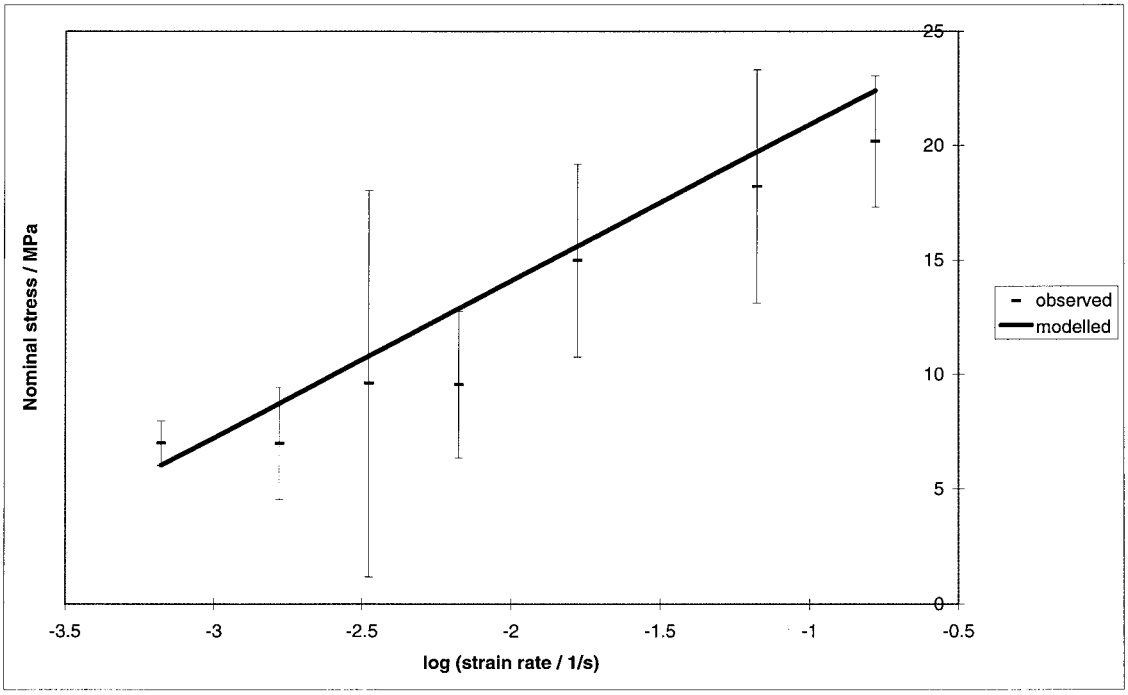


**Figure 10** Rate dependence of yield stress at 75°C.

with the local nature of the instability condition; it can vary between 0.001 and 0.006 without significant consequences.

Results are calculated for a range of $\Delta\dot{\lambda}$ to $\Delta\dot{\lambda} = 0.2\dot{\lambda}$. They are reported in Figures 11–13 in the form of the stress difference $S_1 - S_2$ plotted against $\Delta\dot{\lambda}/\dot{\lambda}$.

In Figure 11, we show a typical result at 80°C, for the applied strain rate of $6.667 \times 10^{-3}$ s$^{-1}$. $S_1 - S_2$ is negative over the range of strain rate, corresponding to a prediction of no necking. This is consistent with observations. All the strain rates at this temperature give similar results.

In Figure 12, the same quantities are plotted for 60°C at the same applied rate. The stress difference $S_1 - S_2$ now becomes positive once the strain rate has been increased by 3%; the same pattern emerges at all testing speeds. Thus, the model predicts a small region of stability followed by instability. It is feasible that natural variations in the strain rate along the length of a specimen would cause fluctuations in rate at the 3% level, and so the prediction is essentially that necking will take place. This is in line with the observations at all rates at this temperature.

At 75°C, the necking predictions vary with rate of strain, as can be seen in Figure 13. The stress

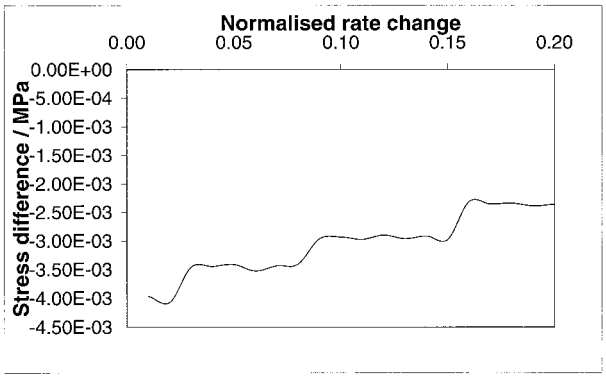


**Figure 11** Necking model results at 80°C at strain rate $6.667 \times 10^{-3}$ s$^{-1}$.

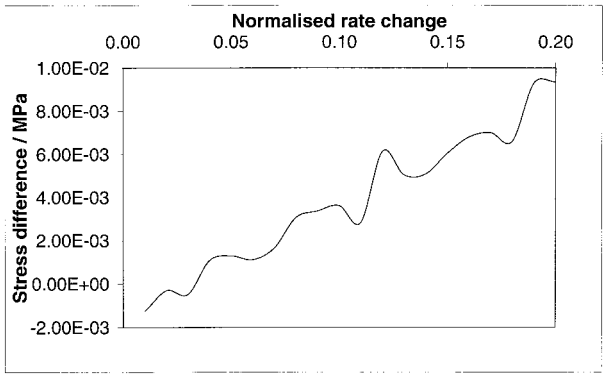


**Figure 12** Necking model results at 60°C at strain rate $6.667 \times 10^{-3}$ s$^{-1}$.

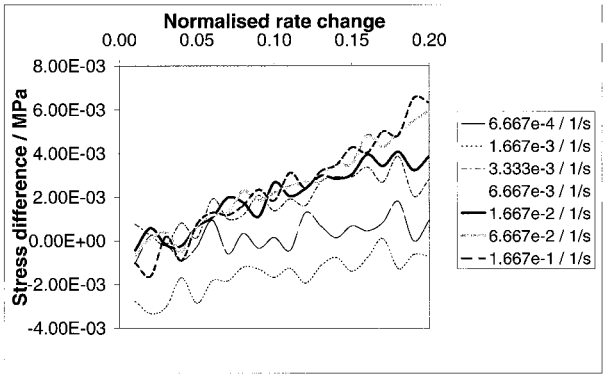


**Figure 13** Necking model results at 75°C for all strain rates.

difference is not a monotonic function of $\Delta\dot{\lambda}/\dot{\lambda}$, probably as a result of numerical errors arising from its smallness, but a clear trend is discernible. At the second slowest speed of $1.667 \times 10^{-3}$ $s^{-1}$, the stress difference is negative over the whole range of $\Delta\dot{\lambda}/\dot{\lambda}$ except at the point $\Delta\dot{\lambda}/\dot{\lambda} = 0.17$; this is a clear prediction of stable behavior. At the lowest speed, the predictions are equivocal, with the stress difference oscillating between negative and positive values. At all higher speeds, of $3.333 \times 10^{-3}$ $s^{-1}$ and greater, there are predictions of necking, although at the rate $6.667 \times 10^{-3}$ $s^{-1}$, the instability is preceded by a stable interval: $0 \leq \Delta\dot{\lambda}/\dot{\lambda} \leq 0.07$. Given the uncertainties involved, the best interpretation is that there will be uniform drawing at low speeds and necking at high speeds, with the transition between the two behaviors occurring between $3.333 \times 10^{-3}$ $s^{-1}$ and $6.667 \times 10^{-3}$ $s^{-1}$. This should be compared with the experimental observations, which are that drawing is stable at rates of $1.667 \times 10^{-2}$ $s^{-1}$ and below and that necking occurs at rates of $3.333 \times 10^{-2}$ $s^{-1}$ and above. This is clearly a significant quantitative error, but not surprising in view of the approximate nature of the modeling of the stress–strain curves.

## CONCLUSIONS

An instability criterion was developed which is equivalent to a minimum-energy condition. It differs from that of Hart[5] but is equivalent to that of Coates and Ward.[6]

The uniaxial stretching behavior of PET can be adequately modeled using a combination of an Eyring process, a Gaussian network, and a linear elastic element. The model is applicable at the three experimental temperatures of 60, 75, and 80°C. It has been used in the implementation of the minimum-energy-based instability criterion. The predictions of the resulting instability model—that necking occurs at 60°C, does not occur at 80°C, and occurs at 75°C only at high speeds—are in line with experimental observations. At 75°C, the speed at which the transition from stable to unstable behavior occurs is captured only roughly by the model. However, the general level of success of the model is surprisingly high, given its simplicity and the level of approximation of the modeling of the stress–strain curves. The instability criterion developed here could be applied to other polymers. It could also be extended to multiaxial states of strain, provided that an appropriate model of polymer deformation were used.

## REFERENCES

1. Allison, S. W.; Ward, I. M. Brit J Appl Phys 1967, 18, 1151–1164.
2. Long, S. D.; Ward, I. M. J Appl Polym Sci 1991, 42, 1921–1929.
3. van der Geissen, E.; de Borst, R. In Material Instabilities in Solids; de Borst, R.; van der Geissen, E., Eds.; Wiley: New York, 1998.
4. Ward, I. M. Mechanical Properties of Solid Polymers, 2nd ed.; Wiley: New York, 1990.
5. Hart, E. W. Acta Metall 1967, 15, 351.
6. Coates, P. D.; Ward, I. M. J Mater Sci 1980, 15, 2897–2914.
7. Campbell, J. D. J Mech Phys Solids 1967, 15, 359–370.
8. Rietsch, F.; Duckett, R. A.; Ward, I. M. Polymer 1979, 20, 1133.
9. Buckley, C. P.; Jones, D. C. Polymer 1995, 36, 3301–3312.
10. Buckley, C. P.; Jones, D. C.; Jones, D. P. Polymer 1995, 37, 2403–2414.
11. Haward, R. N. J Polym Sci Part B Polym Phys 1995, 33, 1481–1494.
12. Sweeney, J.; Ward, I. M. Polymer 1995, 36, 299–308.
13. Arruda, E. M.; Boyce, M. C. Int J Plast 1993, 9, 697–720.